MODELLING FOR OPTIMISATION OF SELF-POWERED WIRELESS SENSOR NODES

P. D. Mitcheson, D. C. Yates, E. M. Yeatman, T. C. Green, A. S. Holmes

Imperial College London, UK

ABSTRACT

Achieving self-powered operation of an implantable sensor is difficult with current technology, despite the fact that the theoretical energy available for harvesting exceeds the theoretical energy required. Moreover, the design and realisation of such sensors nodes is a multi-domain task, requiring global system modelling and optimisation. This paper addresses how such systems can be modelled and optimised by considering both the individual subsystems and their interdependence. The subsystems considered are: an energy-harvesting generator, power converter and a radio link. Optimising these subsystems individually would result in a low overall system performance, but a global optimisation would have too many parameters. In order to make the optimisation and design practical it is suggested that the system is partitioned at the interface betwen the power supply output and the load circuitry, allowing the optimisation to be done in two parts whilst still finding a global optimum. Finally, we consider the dependence of power issues on device size, and show that effective performance from a body sensor node is achievable for a device volume in the cubic millimetres range.

Keywords: Micro-power generator, micropower supply, wireless sensor, ultra-low power radio

1 INTRODUCTION

The fields of ubiquitous computing and medical sensing require ultra-low power, miniaturised, autonomous devices, capable of wireless data transfer. They require a lifetime of many years meaning that batteries are insufficient as the sole power source [1]. Consequently these sensors must harvest energy from their environment using a built-in generator, and additionally the power budget for the load electronics is very limited. The power output from the energy-harvesting generator must be processed to a rail voltage suitable for the load electronics or a secondary cell. Depending upon the implementation of this generator, the power processing electronics may have to convert, with high efficiency, very low or very high voltages, through one or more orders of magnitude, to the rail voltage. The design of the power processing electronics and the effectiveness of the mechanical generator are closely linked and thus a combined optimisation is necessary.

The power consumption of the load electronics is typically dominated by the transceiver. The size constraint presents a unique design challenge for the RF engineer, who must consider the trade-off between antenna efficiency and circuit losses, both of which increase with frequency. Off-the-shelf low-power transceivers can only achieve data rates of tens of bits per second [2] when operated at a sufficiently low duty cycle to be powered from an energy-harvesting generator. Such low data rates are insufficient for key applications such as ECG measurement.

Various different transduction mechanisms are possible when harvesting energy. This work only considers using kinetic energy as the energy source although many other forms are possible [3, 4]. For electrostatic generators which harvest energy from human body motion, the efficiency of the power processing electronics reduces as the rail voltage drops, whereas the power consumption of the transmitter reduces with reducing rail voltage. Consequently, once optimal power electronics and load electronics have been designed across the possible variations in rail voltage, an optimal rail voltage can be found in order to minimise the fraction of generated energy consumed by the load. Any additional energy can be stored for times when the generator is inactive.

2 POWER SUPPLY

The power supply comprises an energy-harvesting generator, power-processing electronics and associated control electronics. The operating principle of the generator is illustrated in Fig. 1, that is, when the frame experiences acceleration (i.e. $\ddot{y}(t) \neq 0$) the inertia of the proof mass causes the mass to move relative to the frame and do work against a damping force. The damping force is implemented using piezoelectric, electromagnetic or electrostatic forces and thus energy dissipated in the damper of this model is the energy that can be converted into an electrical form.

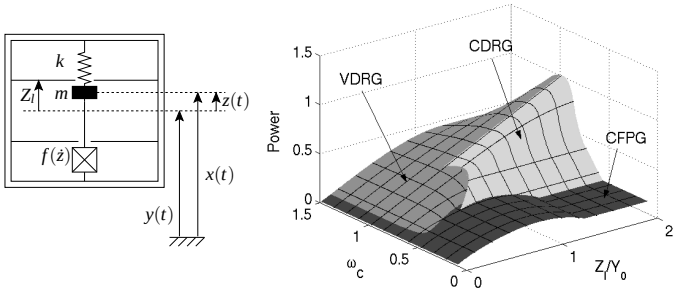

Figure 1: Generalised mechanical modelling.

2.1 Mechanical Modelling

The first considerations for maximising the power density of the generator are concerned with the basic configuration of the generator:

1. How much of the generator volume should the mass occupy?
2. What should the velocity-force characteristic of the damping force be?
3. Should the generator be resonant or non-resonant?

It has been shown that setting the mass to occupy half the volume [5] is optimal for sinusoidal acceleration inputs. Three generator architectures based around the second and third questions were identified in [5] and their performances compared across all operating conditions for the generator, as shown in Fig. 1. The three types are velocity-damped resonant generator (VDRG), coulomb-damped resonant generator (CDRG) and coulomb-force parametric generator (CFPG). The optimal architecture is dependent upon operating condition, and as can be seen from the surface plot of Fig. 1, the CFPG is superior when the generator is small compared to the amplitude of the driving motion. This generator architecture will be used to illustrate the next part of the modelling process. The CFPG is a non-linear, snap-action device [6], where the mass only moves relative to the generator frame near the peak of the frame acceleration, in order to maximise the available force-distance product of the damper, and thus the energy generated.

2.2 Electro-mechanical Modelling

Whilst choosing an architecture is technology independent (within the limits of what can be reasonably implemented), the next stage in design requires a decision on implementation. The CFPG requires a constant (Coulomb) force opposing the relative motion between the mass and frame. The easiest way of achieving such forces in MEMS is with either a parallel plate capacitor operated under constant charge or a comb drive in constant voltage. A parallel plate in constant charge was chosen because higher forces can be achieved per unit volume. The capacitor is charged to low voltage at high capacitance. Energy is generated as the plates separate at constant charge, with the generated energy being captured when the capacitor discharges at minimum capacitance.

In order for the generator to convert as much energy as possible into an electrical form, it is important that the charge placed on the capacitor at low voltage stays in place while the plates separate. Any leakage or charge sharing with parasitic capacitances will reduce the effectiveness. Because the charging and discharging of the capacitor is controlled by semiconductor switches, and increasing the area of these switches will increase their efficiency but decrease the effectiveness of the generator, a combined electro-mechanical simulation is required. The most suitable platform for this simulation work is the circuit simulator SPICE. In order to simulate the generator in SPICE, a behavioural model of the mechanics and electrostatics was created. Part of this, a MEMS capacitor, is shown in Fig. 2.

Results from an electro-mechanical simulation from SPICE are shown in Fig. 3. The top trace shows the behaviour of the mechanics, with the moving plate flying between the limits of travel. The lower trace shows the voltages developed by the generator. This simulation does not include the power processing electronics, although the simulation model presents its output on an electrical port in SPICE meaning that combining the power electronics into the simulation is straight-forward.

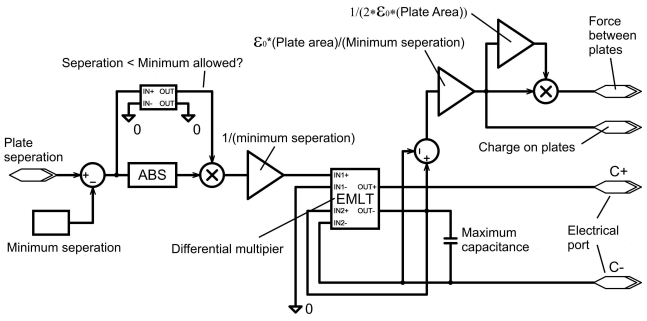

Figure 2: SPICE behavioural model of MEMS capacitor.

2.3 Device Modelling

Custom semiconductor devices capable of switching high voltages at high current density, whilst still presenting minimum parasitic capacitance to the generator, were designed

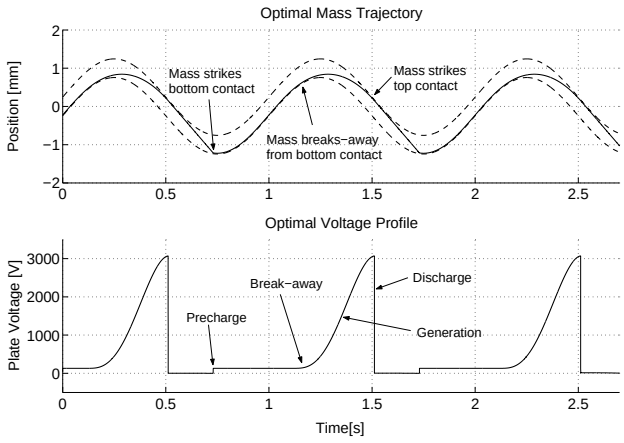

Figure 3: SPICE simulation result.

in a finite-element simulator [7]. Whilst this simulator produces accurate results for semiconductor performance, it is not possible to construct large circuit behavioural models (for example of the generator mechanics). Consequently, the custom semiconductors have to be implemented in SPICE. Fig. 4 shows a SPICE subcircuit model used to simulate a custom designed power MOSFET. It should be noted that the simple SPICE MOSFET model is not sufficiently accurate to describe this device because the standard model does not include JFET pinch at the drain end of the MOS channel. The device models can now be incorporated into the electro-mechanical system model in order to run full simulations of the power supply, and investigate optimal power electronic circuit designs.

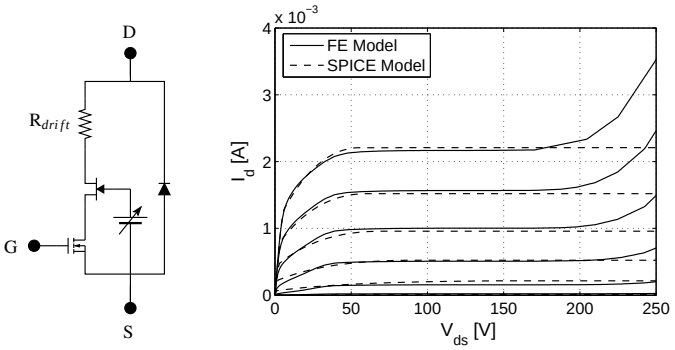

Figure 4: SPICE subcircuit MOSFET model and curve traces.

3 POWER USAGE

The loop antenna is well suited to wireless sensing applications because of its omnidirectional nature, its possible dual use as the inductor in an LC oscillator, and its widespread use in wireless power delivery. Previously a Colpitts oscillator transmitter was reported in which a loop antenna doubled as the inductor in the LC tank [8]. In this work we have developed a design methodology for minimising the power consumption of this type of oscillator transmitter given a constraint on the maximum antenna size [2,9]. Optimisation of the design requires consideration of the desired characteristics of an antenna in conjunction with those of the inductor in an LC oscillator and the frequency dependent losses of the RF MOS transistor.

3.1 Antenna Modelling

The loop antenna has been simulated in MATLAB using a combination of analytical and numerical techniques. Modelling the current distribution and input impedance of the electrically large loop antenna using the method detailed in [10] enables the variation of radiation resistance, directivity, radiation efficiency and Q-factor with the electrical size to be evaluated [2]. It has been shown that, given a certain maximal constraint on the antenna size, the optimal transmission frequency in terms of maximum power transfer from the transmitter antenna input to the receiver load corresponds to an antenna electrical size of approximately 0.2, as shown in fig 5.

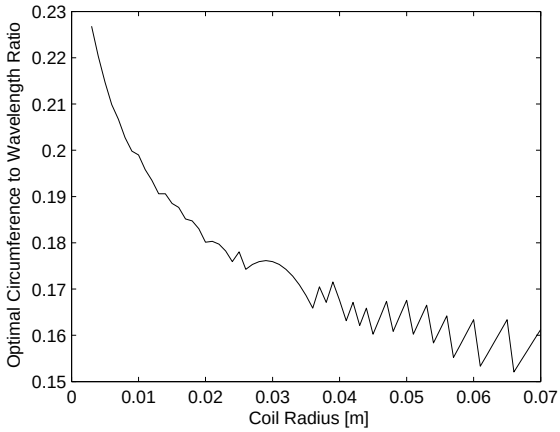

Figure 5: Optimal electrical size of loop antenna.

3.2 Device and Circuit Modelling

RF circuits and devices are usually modelled using specialised circuit simulators such as Cadence's SPECTRE RF (see transient simulation example in Fig. 6). Such a simulator is unfortunately not suited to this optimisation, since the range and number of variables is simply too large. Each specific set of parameters requires a separate transient, periodic steady-state and periodic noise analysis, which all need considerable computing time. Furthermore, these simulations normally need tweaking by the user to achieve meaningful results, making automation of such an optimisation process impractical.

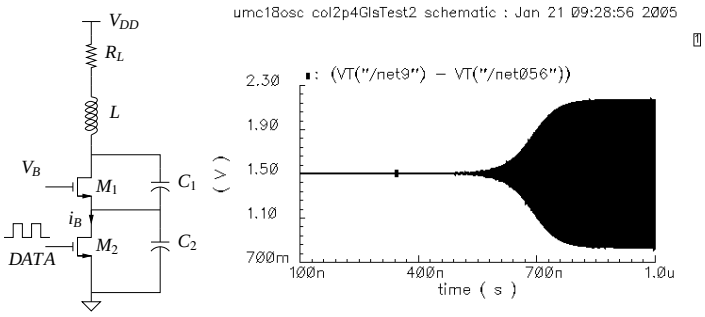

Figure 6: Oscillator circuit and start up transient.

The RF circuits and devices have thus also been modelled in MATLAB using a combination of analytical and numerical techniques. The EKV model [11] has been used in conjunction with a high frequency model presented in [12] to model the transistor (see Fig. 7). The required bias current for a particular

oscillation voltage, given the antenna dimensions and operating frequency, has been evaluated using an energy conservation technique. The MATLAB simulations were compared with SPECTRE RF for specific circuit and device parameters to improve the accuracy.

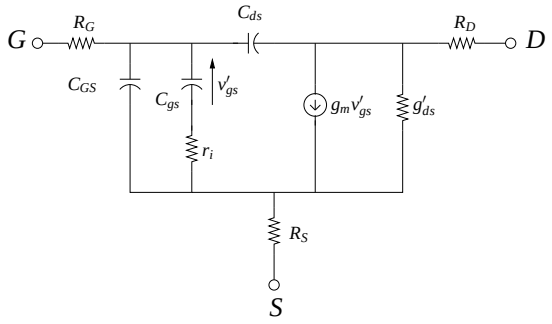

Figure 7: High frequency MOSFET model.

3.3 Combined Optimisation

Figure 8 shows the preferred carrier frequency from the standard ISM bands for a given maximum allowed antenna size. This has been found by combining the antenna, circuit and device analyses. The oscillation voltage needed for successful data transfer has been calculated by simple manipulation of the well known Friis transmission formula combined with modelling of the oscillator linewidth using [13].

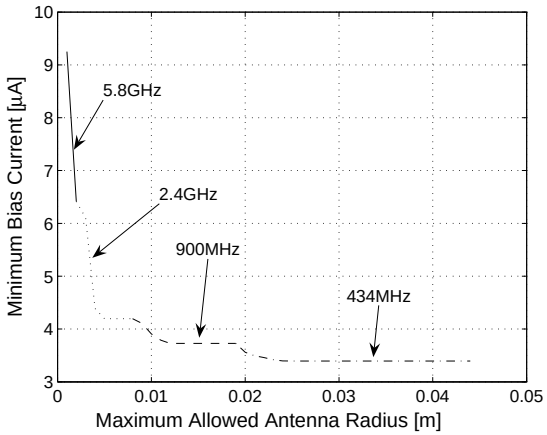

Figure 8: Minimum bias current for data transfer.

4 GLOBAL OPTIMISATION

Previously [5] we have shown that the generator output depends on the excitation amplitude Y_0 and frequency ω, internal displacement Z_l and proof mass m, according to:

$$P \approx \frac{1}{2} Y_0 Z_l \omega^3 m \tag{1}$$

This holds for the CFPG or for resonant devices operating at resonance. Let us now assume for the generator shape a flat square of dimensions $a \times a \times \alpha a$ where $\alpha << 1$. This form will support an antenna coil of radius $a/2$. The optimal mass will occupy approximately half the volume [14] leaving an internal displacement amplitude $a/4$. Then for a proof mass density ρ, substituting $Y_0\omega^2$ for the maximum external acceleration A_0, we have:

$$P \approx \frac{1}{16} A_0 \omega \rho \alpha a^4 \tag{2}$$

A peak acceleration of about 1g (10m/s^2) is typical of body motion [14] at about 1 Hz. Then, taking an aspect ratio, $\alpha = 0.1$ and $\rho = 2 \times 10^4$ kg/m^3 (gold), we obtain

$$P \approx 8 \times 10^3 a^4 \text{ W/m}^4 \tag{3}$$

Note that (for $\alpha = 0.1$) we can write this as:

$$P \approx 1.7 V^{4/3} \text{ mW/cm}^4 \tag{4}$$

where V is the generator volume.

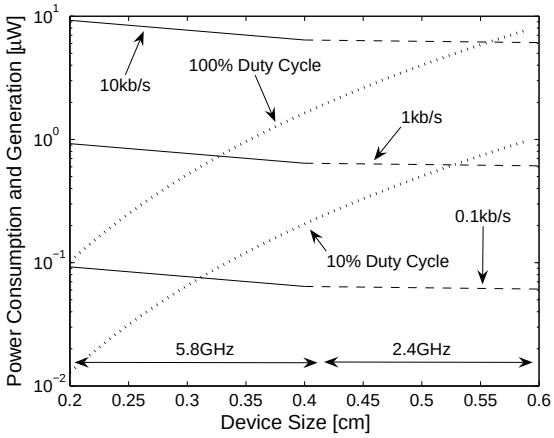

Figure 9: Comparison of power generation with power consumption as a function of device size and data rate. Minimum power consumption as solid/dashed lines and maximum power generation capability as dotted lines. Optimal transmission frequency changes at a device size of 4 mm. The receiver noise figure is 20 dB and the radio link is assumed to operate over a 1 m distance.

The bias current results of Fig. 8 are easily converted to approximate power consumption values for the transmitter by multiplying by V_{DD}. Correct operation of the switches M_1 and M_2 require V_{DD} to be large enough to drive both MOSFETS into saturation, so we choose V_{DD} = 1V. The average power consumption also scales with transmitter duty cycle (assuming negligible power during rest state). Meanwhile power generation scales with antenna radius according to 3 and using $r = a/2$. We can also introduce a duty cycle for generation, corresponding to the fraction of time when external motion is available for generation. In Fig. 9 we plot transmitter power and generator output for several duty

cycles of both transmitter and generator. The crossing points indicate the minimum size of the sensor node, assuming the generator dominates the size. It can be seen that, for example, with 10% generator duty cycle and an average transmission rate of 0.1 kb/s, the minimum device dimension is 3 mm, so that with the assumed aspect ratio $\alpha = 0.1$ we have a generator volume of ≈ 10 mm^3, or 0.01 cc, a size that is not excessive for many body sensor applications. This device size is a lower bound because a small amount of power will be required for control and sensing electronics.

5 CONCLUSIONS

We have described a number of issues associated with optimisation of functional blocks in a self-powered body sensor node, and shown a number of interactions between these that require an integrated approach to design and optimisation. By considering the dependence of both transmitter power consumption and generator output power on device dimensions, we have shown that effective performance from a body sensor node is achievable for a device volume of 10 cubic millimetres.

References

[1] E. M. Yeatman, "Advances in Power Sources for Wireless Sensor Nodes," in *International Workshop on Wearable and Implantable Body Sensor Networks Proceedings*, Imperial College London, U.K., April 2004.

[2] D. C. Yates, A. S. Holmes, and A. J. Burdett, "Optimal transmission frequency for ultralow-power short-range radio links," *IEEE Transactions on Circuits and Systems Part 1*, vol. 51, no. 7, pp. 1405–1413, July 2004.

[3] S. Roundy, P. K. Wright, and J. M. Rabaey, *Energy Scavenging for Wireless Sensor Networks*, 1st ed. Boston, Massachusetts: Kluwer Academic Publishers, 2003.

[4] T. Starner and J. A. Paradiso, "Human Generated Power for Mobile Electronics," in *Low Power Electronics Design*, C. Piquet, Ed. CRC Press, 2004, to be published.

[5] P. D. Mitcheson, T. C. Green, E. M. Yeatman, and A. S. Holmes, "Architectures for Vibration-Driven Micropower Generators," *IEEE/ASME Journal of Microelectromechanical Systems*, vol. 13, no. 3, pp. 429–440, June 2004.

[6] P. D. Mitcheson, P. Miao, B. H. Stark, E. M. Yeatman, A. S. Holmes, and T. C. Green, "MEMS Electrostatic Micro-Power Generator for Low Frequency Operation," *Sensors and Actuators, part A*, vol. 115, no. 2–3, pp. 523–529, 2004.

[7] B. H. Stark, P. D. Mitcheson, P. Miao, T. C. Green, E. M. Yeatman, and A. S. Holmes, "Power processing issues in electrostatic micro-power generators," in *35th IEEE Annual Power Electronics Spoecialists Conference*, Aachen, Germany, 2004, pp. 4156–4162.

[8] B. Ziaie, K. Najafi, and D. J. Anderson, "A low-power miniature transmitter using a low-loss silicon platform for biotelemetry," in *Proc. 19th IEEE International conference of Engineering in Medicine and Biology Society*, vol. 5, 1997, pp. 2221–2224.

[9] D. C. Yates and A. S. Holmes, "Loop antenna design for ultra low power transmitters," in *IEEE International Workshop on Antenna Technology, Singapore*, 2005, accepted.

[10] R. W. P. King and G. S. Smith, *Antennas in matter: Fundamentals, theory and applications*. Cambridge, MA: MIT Press, 1981.

[11] C. C. Enz, F. Krummenacher, and E. A. Vittoz, "An analytical MOS transistor model valid in all regions of operation and dedicated to low-voltage and low-current applications," *Analog Integrated Circuits and Signal Processing*, pp. 83–114, July 1995.

[12] T. Manku, "Microwave CMOS - device physics and design," *IEEE Journal of Solid State Circuits*, vol. 34, no. 3, pp. 227–285, March 1999.

[13] D. Ham and A. Hajimiri, "Virtual damping and Einstein relation in oscillators," *IEEE Journal of Solid State Circuits*, vol. 38, no. 3, pp. 407–418, March 2003.

[14] T. von Büren, P. D. Mitcheson, T. C. Green, E. M. Yeatman, A. S. Holmes, and G. Tröster, "Optimization of Inertial Micropower Generators for Human Walking Motion," *IEEE Sensors Journal*, 2005, in press.